Macromolecules

Article

pubs.acs.org/Macromolecules

Self-Assembly Behavior of Thermoresponsive Bis-Solvophilic Linear Block Terpolymers: A Simulation Study

Othonas Moultos,[†] Leonidas N. Gergidis,[‡] and Costas Vlahos[†,*]

[†]Department of Chemistry, University of Ioannina, 45110 Ioannina, Greece

[‡]Department of Materials Science & Engineering, University of Ioannina, 45110 Ioannina, Greece

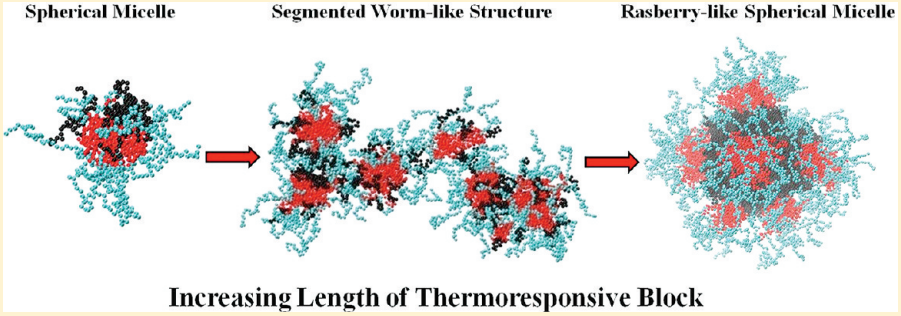

ABSTRACT: The micellization behavior of linear ABC terpolymers containing a solvophobic block in the middle, accompanied by solvophilic and thermoresponsive blocks at the ends, is studied by means of Brownian dynamics simulations. The effects of the length of the thermoresponsive moiety on the shape and size of aggregates, formed as the temperature of the solution reduces and solvent progressively becomes bad for the thermoresponsive block, are studied in detail. Two crossover temperatures, $T^* = 2.4$ and $T^* = 2.0$, were found. The first one corresponds to the formation of loose aggregates and the second one to regular micelles. At both solution temperatures, as the thermoresponsive block length increases, a shape transition from spherical to segmented worm-like and back to spherical loose aggregates or micelles was observed. Our results are compared with recent experimental findings of similar systems.

1. INTRODUCTION

The self-assembly of amphiphilic AB diblock copolymers in solution into spherical or cylindrical micelles, has attracted much attention in recent years due to their potential applications in nanotechnology, cosmetics, paints and drug delivery systems.[1,2] The effects of architecture, molecular weight, and the stiffness of the blocks on the micelle's shape and size as well as the ones of the chemical mismatch between the blocks have been studied extensively by theory and experiments in the past few years and are relatively well understood.[3−8]

As the number of distinct blocks increases from two to three, for example, ABA linear triblock copolymers and ABC linear terpolymers, both the complexity and the variety of self-assembled structures significantly increase. In the case of linear ABA terpolymers built from two solvophobic A blocks on the sides and a solvophilic B block in the middle, flower-like micelles are obtained at low copolymer concentration while thermodynamic geletion is observed at higher concentrations.[9,10] Linear amphiphilic ABC terpolymers, containing two different solvophilic A, C blocks at the sides and a solvophobic B block, form a plethora of complex vesicle shapes or spherical micelles with mixed, patchy or Janus-like corona depending on the tuning of interaction parameters between the different blocks and their relative lengths.[11,12] Linear terpolymers of the opposite nature, containing a solvophilic A block at the one end and two successive solvophobic blocks B and C, form multicompartment core, raspberry-like, worm-like, or comb-like micelles.[13,14]

An interesting category of ABC terpolymers are those containing an environmentally sensitive polymeric block. These terpolymers exhibit large, sharp changes in response to physical stimuli (such as temperature, solvent, or light) or to chemical stimuli (such as pH, ions in solution, or chemical recognition). Responses differ depending on the stimulus applied and may include changes in shape, volume or mechanical properties among others. These terpolymers involved in a variety of interesting applications for encapsulation, for controlled delivery, or as "intelligent" switches among them.[15−18]

Walther et al.[19] have synthesized and studied a series of bishydrophilic block terpolymers, with a poly(*n*-butyl acrylate) (PnBuA) as hydrophobic middle block and poly(ethylene oxide) (PEO) and poly(*N*-isopropylacrilamide) (PNiPAAm) as outer blocks. PNiPAAm is a thermoresponsive polymer with lower critical solution temperature (LCST), behavior exhibiting cloud points just below the human body temperature (32 °C). Cryo-TEM and light scattering measurements showed that the collapse of PNiPAAm block triggers the clustering of micelles

Received: November 23, 2011
Revised: February 2, 2012
Published: February 22, 2012

into superstructures when the contour length of the thermoresponsive block is longer than the one of the hydrophilic PEO polymer. Several heating cycles from 25 to 45 °C showed an increase in the amount of micelles from mainly mixed micelles into micelles with preferentially two opposing sticky patches. This gives rise to a linear assembly of segmented worms and comb like micelles. A full transition to the Janus-like micelles and consequently to spherical superstructures does not take place.

At temperatures higher than the LCST of PNiPAAm the micellization behavior of the aforementioned terpolymer should be more or less similar to an ABC terpolymer's composed of solvophilic−solvophobic−solvophobic blocks when the interactions between different units are similar. Li et al.[20] studied ABC miktoarm star terpolymers composed of two hydrophobic (poly(ethylethylene), poly(methylcaprolactone)) and one hydrophilic (poly(ethylene oxide)) branches. In contrast, they found that when the poly(methylcaprolactone) arm increases results in a transition from spherical micelles to segmented worms and to spherical superstructures. The latter transition can be attributed on the assembly of sticky patchy Janus type segments.

Despite the aforementioned potential of thermoresponsive ABC terpolymers in applications the theoretical and experimental studies reported in the literature are restricted. We employed Brownian dynamics simulations in order to elucidate the effects of the thermoresponsive block and the system temperature on the micellization behavior. Brownian dynamics has successfully been used in the study of self- assembly of various copolymers and it is expected to be also appropriate for the study of linear ABC terpolymers.[6−8,21] The properties of interest are the preferential aggregation number (N_{ag}) and the shape of the micelle which is expressed by the shape anisotropy parameter (κ^2) and the mean square radius of gyration ($\langle R_g^2 \rangle$) of the solvophobic core, of the corona, and of the whole micelle. In addition, we report direct comparisons of our simulation results with experimental findings of similar systems existing in the literature.[19,20]

2. MODEL

We employed a coarse-grained model in order to study the amphiphilic terpolymers. A group of atoms was modeled as a bead (with diameter σ), while different beads were connected with flexible finitely extended elastic bonds (FENE). The FENE potential is expressed as

$$U_{Bond}(r_{ij}) = \begin{cases} -0.5kR_0^2 \ln\left[1 - \left(\frac{r_{ij}}{R_0}\right)^2\right], & r_{ij} \le R_0 \\ \infty, & r_{ij} > R_0 \end{cases} \quad (1)$$

where r_{ij} is the distance between beads i and j, $k = 25T\varepsilon/\sigma^2$, and R_0 is the maximum extension of the bond ($R_0 = 1.5\sigma$). These parameters[21,22] prevent chain crossing by ensuring an average bond length of 0.97σ. Monomer−monomer interactions were calculated by means of a truncated and shifted Lennard-Jones potential

$$U_{LJ}(r_{ij}) = \begin{cases} 4\varepsilon_{ij}\left[\left(\frac{\sigma}{r_{ij}}\right)^{12} - \left(\frac{\sigma}{r_{ij}}\right)^{6} - \left(\frac{\sigma}{r_{cij}}\right)^{12} + \left(\frac{\sigma}{r_{cij}}\right)^{6}\right] \\ \quad + \varepsilon_{ij}, \quad r_{ij} \le r_{cij} \\ 0, \quad r_{ij} > r_{cij} \end{cases} \quad (2)$$

where ε_{ij} is the well-depth and r_{cij} is the cutoff radius. The solvent molecules are considered implicitly. The short time-steps needed to model solvent's behavior (the fast motion) restrict the time scales that maybe sampled, thereby limiting the information that can be obtained for the slower motion of the copolymer. Brownian dynamics simulation method allows the statistical treatment of the solvent, incorporating its influence on the copolymer by a combination of random forces and frictional terms. The friction coefficient and the random force couple the simulated system to a heat bath and therefore the simulation has canonical ensemble (NVT) constraints. The equation of motion of each bead i of mass m in the simulation box follows the Langevin equation:

$$m_i\ddot{\boldsymbol{r}}_i(t) = -\nabla \sum_j [U_{LJ}(r_{ij}) + U_{Bond}(r_{ij})] - m_i\xi\dot{\boldsymbol{r}}_i(t) + \mathbf{F}_i(t) \quad (3)$$

where m_i, $\boldsymbol{r}_i$, and ξ are the mass, the position vector, and the friction coefficient of the i bead, respectively. The friction coefficient is equal to ξ=0.5τ^{-1}, with $\tau = \sigma(m/\varepsilon)^{1/2}$. The random force vector $\boldsymbol{F}_i$ is assumed to be Gaussian, with zero mean, and satisfies the equation

$$\langle \mathbf{F}_i(t)\cdot\mathbf{F}_j(t')\rangle = 6k_BTm\xi\delta_{ij}\delta(t - t') \quad (4)$$

k_B is the Boltzmann constant and T is the temperature.

We constructed linear ABC terpolymers of the type $A_{NA}B_{30}A_{NC}$, with solvophilic A units, solvophobic B and thermoresponsive C units as typically shown in Figure 1. In

Figure 1. Cartoon representation of $A_5B_5C_5$ terpolymer.

all conducted simulations both the solvophobic part B and the solvophilic part A of terpolymers contained 30 beads, while the length of the thermoresponsive block varied containing N_c = 3, 5, 10, 15, 30, and 45. The Brownian dynamics simulations were performed in a cubic box with periodic boundary conditions, using the open-source massive parallel simulator LAMMPS.[23,24] Previous works have proved the high efficiency of LAMMPS in the study of amphiphilic copolymers.[6−8,21] The reduced temperature of the simulation $T^* = k_BT/\varepsilon$ varied from T^* = 4.0 (good solvent) to T^* = 3.0 (Θ solvent), 2.8, 2.6, 2.4, 2.2, 2.0 (bad solvent) and T^* = 1.8 (deep inside the biphasic area). Different cutoff distances and epsilon parameters (ε_{BB}= T^*/1.8, $\varepsilon_{ij} = \varepsilon$, for i,j ≠ B) in the Lennard-Jones potential were used[21,22] to describe the interactions between copolymer units. The A−A, A−B, A−C, and B−C interactions were considered repulsive

dx.doi.org/10.1021/ma2025573 | Macromolecules 2012, 45, 2570−2579

and have cutoff radii $r_{cij} = 2^{1/6}\sigma$ while the B−B interaction had an attractive potential with cutoff radius $r_{cij} = 2.5\sigma$. With the chosen interaction parameters the A units will remain under good solvent conditions and the B under bad solvent conditions despite the temperature changes. The solvent conditions for the thermoresponsive block C (C−C interactions) varied from good to Θ and progressively to bad solvent. For the sake of simplicity, all types of beads were considered to have the same mass ($m = 1$) and diameter ($\sigma = 1$).

In the present work, systems with 1000 polymeric chains were simulated. Amphiphiles at reduced temperatures T^* higher than the order−disorder transition temperature of the thermoresponsive moiety (UCST in the simulations) were assumed to reside to the same micelle if the distance between any two nonbonded solvophobic beads B, belonging to different chains, was found within 1.5σ. The aforementioned criterion has been adopted by the literature for the description of the micellization process where this distance corresponds to the maximum extension of the FENE bonds.[21] At reduced temperatures T^* close to or smaller than the order−disorder transition temperature of the thermoresponsive block we have secondary aggregation and different micelles are connected to form larger aggregates. Thus, the 1.5σ criterion were also applied for the distance between any two nonbonded C type units, belonging to different terpolymer chains. The choice of $\varepsilon_{BB} = T^*/1.8$ allows the studied systems to have both micelles and free molecules[21] at the reduced temperatures where no secondary aggregation due to thermoresponsive moieties is observed. If the ε_{BB} value is very high, the studied system contains only aggregates and no free molecules; while if it is very low, the studied system contains only free molecules and no aggregates. The system size was chosen so to prevent the largest micelles from having a radius of gyration greater than the one-fourth of the box side length. The use of the one-quarter of the simulation box side proved to be a sufficient condition to avoid interaction of chains and micelles with their images. In all simulations, we set $\varepsilon = 1$.

In order to avoid bond crossing at the desired concentration, the ABC terpolymer molecule was arranged on a lattice box. The energy of the chain was minimized and then the small system was replicated $N_{Polymer}$ times, equal to the number of polymer chains. We performed 1 million time steps with time step 0.008τ setting all cutoff radii equal to $r_{cij} = 2^{1/6}\sigma$ in order to eliminate any bias introduced from the initial conformation. The system then was allowed to equilibrate for 5 million steps. The simulation subsequently conducted for 100 million steps with time step 0.001τ to 0.006τ. This run time corresponds to 0.1−0.6 μs. The length of the simulation was evaluated by calculating the tracer autocorrelation function

$$C(t) = \frac{\langle N(t_o + t)N(t_o)\rangle - \langle N(t_o)\rangle^2}{\langle N^2(t_o)\rangle - \langle N(t_o)\rangle^2} \quad (5)$$

where $N(t)$ is the number of molecules in the micelle in which the copolymer resides at time t. We took all copolymers as tracers, and every time step as a time origin t_0. The characteristic relaxation time t_{relax} is defined as the required time for $C(t)$ to reach the value of e^{-1}. Each simulation was conducted for at least $10t_{relax}$ in order to have 10 independent conformations. Every production run was submitted on 14 processors in a parallel machine with Opteron 2.2 GHz CPU's, and needed about 3−4 weeks time to be completed. The properties of interest were calculated as averages from 1000 snapshots,[7,8] at the concentration [X] = 0.12 where most aggregates are formed.

3. RESULTS AND DISCUSSION

The simulated systems in the present study consisted of a series of ABC terpolymers with one inner solvophobic (B) and two outer solvophilic (A) and thermoresponsive (C) blocks. The terpolymers were of the type $A_{30}B_{30}C_{Nc}$ with 30 solvophilic, 30 solvophobic and a varied number of thermoresponsive units (N_c = 3, 5, 10, 15, 30 and 45). Thus, the lengths of the thermoresponsive block are shorter, comparable to or longer than the solvophilic block, respectively. Consequently the terpolymer systems mentioned above allow a systematic study of the effect of the thermoresponsive block length on the aggregation and the shape of the resulting micelles. According to our calculations of the Kuhn lengths presented in section 4 (Comparison with Experiments) micelles with larger sizes were obtained experimentally in terpolymers with half the thermoresponsive block length compared to the respective solvophilic which is similar to our $A_{30}B_{30}C_{15}$ terpolymers.

3.1. $A_{30}B_{30}C_{15}$ Terpolymer. Our simulation results for the mass distribution of micelles formed by the $A_{30}B_{30}C_{15}$ terpolymers are illustrated in Figure 2 for different solution

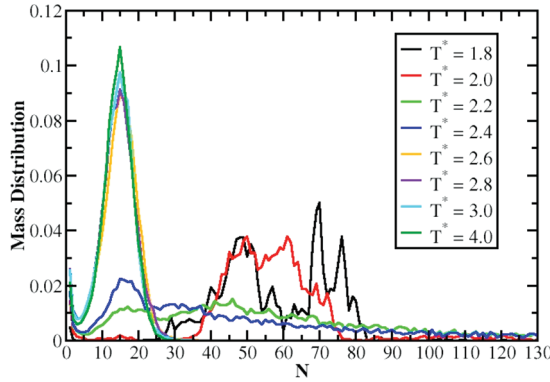

Figure 2. Mass distribution of aggregates for $A_{30}B_{30}C_{15}$ terpolymer at various solution temperatures T^*.

temperatures T^*. The radii of gyration, the shape anistotropy parameter κ^2, of the core, the thermoresponsive units and the whole micelle are presented in Table 1. In every solution temperature examined, the cross interactions between A−B, A−C, and B−C were always considered repulsive while the B−B, with chosen $\varepsilon_{BB} = T^*/1.8$, were very attractive deep inside the biphasic area where the B polymer melts. At $T^* = 4.0$, both solvophilic A and thermoresponsive C units are under good solvent conditions, forming micelles with mixed corona, while the solvophobic B units form the core. In Figure 2, one can observe that the mass distribution of micelles is bell-shaped with most probable aggregation number N_{ag}=15. The shape of the most probable micelle is spherical with shape anisotropy parameter $\kappa^2 = 0.0319$.

Lowering the solution temperature to $T^* = 3.0$, which is Θ for the thermoresponsive block C, the chemical mismatch between A and C units, expressed by the Flory χ_{AC} parameter, increases. This increase is not adequate to change the most probable aggregation number of micelles which remains equal to 15. However, the mean square radius of gyration of the whole micelle is slightly affected and increases from 70.5 to

dx.doi.org/10.1021/ma2025573 | Macromolecules 2012, 45, 2570−2579

Table 1. Shape Characteristic Properties for $A_{30}B_{30}C_{15}$ Terpolymer Aggregates[a]

	T^*	$\langle R_g^2\rangle_{mic}$	$\langle R_g^2\rangle_{solvophobic}$	$\langle R_g^2\rangle_{thermoresponsive}$	$\langle \kappa^2\rangle_{mic}$	$\langle \kappa^2\rangle_{solvophobic}$	$\langle \kappa^2\rangle_{thermoresponsive}$
N_{ag} = 15	4.0	70.5 (0.2)	22.8 (0.2)	69.3 (0.1)	0.0319 (0.0008)	0.098 (0.003)	0.078 (0.002)
	3.0	72.2 (0.3)	23.9 (0.3)	68.5 (0.4)	0.0340 (0.0007)	0.105 (0.002)	0.089 (0.002)
	2.8	72.3 (0.2)	23.9 (0.1)	67.5 (0.3)	0.0345 (0.0008)	0.106 (0.003)	0.093 (0.002)
N_{ag} = 16	2.6	75.0 (0.5)	25.4 (0.4)	68.7 (0.6)	0.035 (0.001)	0.113 (0.004)	0.097 (0.003)
N_{ag} = 29	2.4	153.0 (3.8)	102.4 (4.4)	129.3 (5.0)	0.24 (0.02)	0.50 (0.02)	0.29 (0.02)
	2.2	147.6 (6.3)	96.6 (6.2)	113.4 (6.2)	0.21 (0.01)	0.47 (0.02)	0.27 (0.02)
	2.0	131.4 (5.6)	79.3 (4.3)	65.8 (11.9)	0.16 (0.03)	0.39 (0.06)	0.18 (0.06)
N_{ag} = 47	2.4	245.3 (7.9)	192.5 (8.5)	216.0 (10.0)	0.28 (0.01)	0.46 (0.03)	0.35 (0.02)
	2.2	204.4 (15.3)	148.1 (16.2)	155.5 (19.7)	0.21 (0.04)	0.39 (0.05)	0.29 (0.05)
	2.0	150.4 (1.1)	93.4 (0.7)	63.9 (4.0)	0.09 (0.01)	0.22 (0.03)	0.11 (0.02)
N_{ag} = 50	2.0	155.2 (1.7)	97.7 (2.1)	65.8 (3.7)	0.08 (0.01)	0.18 (0.03)	0.11 (0.01)
N_{ag} = 61	2.0	173.8 (6.9)	113.3 (7.5)	73.8 (10.6)	0.08 (0.02)	0.16 (0.04)	0.12 (0.05)
N_{ag} = 70	1.8	172.8 (8.3)	112.6 (9.2)	48.1 (8.9)	0.04 (0.03)	0.07 (0.04)	0.10 (0.04)
N_{ag} = 76	2.4	420.5 (33.3)	365.7 (33.6)	387.2 (31.8)	0.31 (0.06)	0.41 (0.06)	0.36 (0.06)
	2.2	380.2 (33.1)	323.2 (34.4)	327.8 (38.2)	0.32 (0.06)	0.43 (0.06)	0.41 (0.05)
	2.0	302.1 (63.9)	243.5 (68.3)	210.6 (79.3)	0.3 (0.1)	0.4 (0.1)	0.5 (0.2)
	1.8	195.1 (37.3)	133.4 (38.5)	69.7 (45.7)	0.10 (0.05)	0.10 (0.05)	0.20 (0.05)

[a]Standard deviation is inside the parentheses.

72.2. The respective shape anisotropy parameter κ^2 increases from 0.0319 to 0.0340. Similar trends are also obtained at the solution temperature $T^* = 2.8$. A small increase in the micelles' most probable aggregation number (N_{ag} = 16) is observed in lower solution temperature $T^* = 2.6$. The Flory χ_{AC} parameter increases further and this results in a small increase in the total micelles mean square radius of gyration ($\langle R_g^2\rangle$ = 75.0) and on the respective shape anisotropy parameter κ^2= 0.035.

There are some interesting experimental studies on the aggregation behavior of thermoresponsive PEO−PNIPAAm diblock copolymers in aqueous solutions below the critical micelle temperature (CMT).[25] Since water is a good solvent for both moieties, at lower temperatures (LCST) PEO−PNIPAAm were usually considered to exist as single chains. However, aggregation of PEO−PNIPAAm in aqueous solution at temperatures below its cloud point (32 °C) was observed. This aggregation started at 15 °C, which is 17 °C below the cloud point. The formation of such loose aggregates decreases the free energy of the system since the PNIPAAm blocks get closer, reducing the interaction strength with the solvent and thus increasing the more favored homointeractions.

In Figure 3, we present our Brownian dynamics simulation results for the mean square radius of gyration of thermoresponsive block for a single ABC terpolymer chain at various solution temperatures. All the interaction parameters were the same with the respective parameters of the more concentrated systems. Three different regimes, with two crossover solutions temperatures at $T^* = 2.4$ and $T^* = 2.0$, can be observed. A possible explanation for the regime started at $T^* = 2.4$ could be the end-group effect. It is known that the hydrophobic end group could decrease the solubility and induce the aggregation of the solvophilic polymer, especially in the case that the overall molecular weight of the amphiphilic polymer is relatively low. In the current study we consider that the loose aggregates started to form at this temperature. Thus, for solution temperatures equal to or lower than $T^* = 2.4$, we modified the micellization criterion used for higher solution temperatures. According to the new criterion, two chains reside to the same micelle if the distance between any two nonbonded solvophobic beads B or the distance between any two nonbonded thermoresponsive beads C, belonging to different

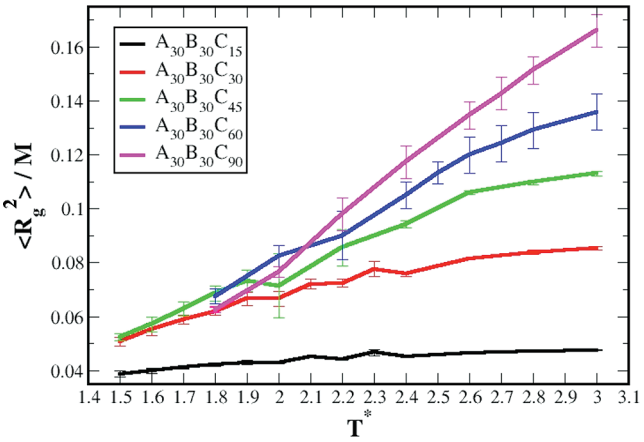

Figure 3. Mean square radius of gyration $\langle R_g^2\rangle$ normalized with the molecular weight M of the thermoresponsive block for various ABC single chain terpolymers with respect to the solution temperatures T^*.

chains, was found within 1.5σ. At $T^* = 2.4$ (Figure 2) the decrease in solubility of the thermoresponsive block triggers the clustering of a significant part of initial micelles (Figure 4a) into new hyper-structures. Snapshot analysis presented in Figure 4 shows the formation of segmented worm-like (Figure 4b, c, d) and comb-like (Figure 4e) loose aggregates connected through thermoresponsive stickers with a wide range of aggregation numbers. The radius of gyration and the shape anisotropy parameter confirm these conclusions. The mean square radius of gyration (Table 1) of hyper-structures with aggregation numbers N_{ag} = 29, 47, 76 are $\langle R_g^2\rangle$ = 153, 245, 420 which are 2, 3, and 5 times higher than the respective radius of gyration of the initial micelle ($\langle R_g^2\rangle$ = 76) with aggregation number N_{ag} = 15. The shape anisotropy parameter κ^2 of the whole aggregate has values 0.046, 0.236, 0.285, and 0.313 for aggregates with N_{ag} = 15, 29, 47, and 76 respectively, indicating a non spherical conformation. In solution temperature $T^* = 2.2$ more of the initial micelles were connected to form hyper-structures. For comparison purposes we have calculated the conformational properties of loose aggregates with the same aggregation numbers as before (N_{ag} = 29, 47, and 76). Both, mean square radius of gyration ($\langle R_g^2\rangle$ = 148, 204, 380) and shape anisotropy

dx.doi.org/10.1021/ma2025573 | Macromolecules 2012, 45, 2570−2579

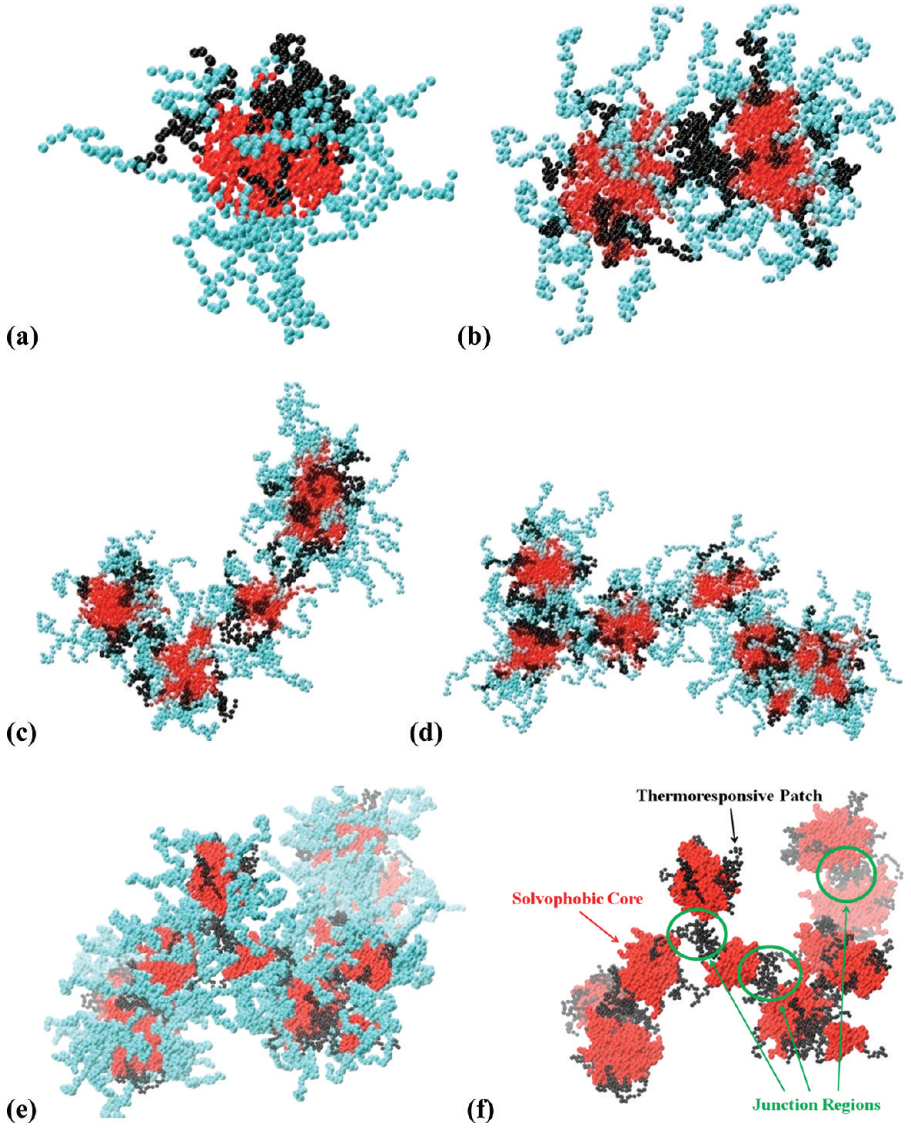

Figure 4. Snapshots of aggregates formed by $A_{30}B_{30}C_{15}$ terpolymer, at $T^* = 2.4$, with aggregation numbers (a) $N_{ag} = 15$, (b) $N_{ag} = 31$, (c) $N_{ag} = 62$, (d) $N_{ag} = 92$, (e) $N_{ag} = 171$, and (f) $N_{ag} = 171$ with solvophilic beads excluded for clarity.

parameter values (κ^2 = 0.211, 0.210, 0.319) were slightly smaller compared to the respective ones at temperature $T^* = 2.4$.

At temperature $T^* = 2.0$, the thermoresponsive block starts to melt and micelles with raspberry-like core (thermoresponsive units in the interior with hydrophobic patches attached on the periphery as shown in Figure 5a,b) are obtained with preferential aggregation numbers N_{ag} = 50 and 61. Snapshot analysis initially revealed the formation of segmented worm like hyper-structures connected through thermoresponsive stickers. Then with the evolution of time these segmented worm-like micelles were wrapped and new spherical micelles with raspberry-like cores were obtained. This shape transition takes place due to the rearrangement of the thermoresponsive blocks which form the interior part of micelles' core. In this mixed core the outer patches are formed by the solvophobic blocks surrounded by the solvophilic corona. The shape anisotropy parameter values for the micelles with the preferential aggregation numbers N_{ag} = 50 and 61 are κ^2= 0.077, 0.077 respectively, clearly indicating a spherical conformation. At the lowest solution temperature examined in the present study ($T^* = 1.8$) all micelles formed were spherical with raspberry-like core, similar to the ones presented in Figure 5c. We should notice here that there was significant population of micelles with aggregation numbers N_{ag}= 70, 76 higher than the ones in the previous temperature $T^* = 2.0$.

3.2. $A_{30}B_{30}C_{30}$ Terpolymer. Next we studied the amphiphilic terpolymers $A_{30}B_{30}C_{30}$ where the thermoresponsive C block contained the same number of beads with the solvophilic A block. Our results for the micelles mass distribution are illustrated in Figure 7 while the values of their size and shape are presented in Table 2. At solution temperature $T^* = 4.0$, where the thermoresponsive block is under good solvent conditions, only spherical micelles (κ^2 = 0.028, $\langle R_g^2 \rangle$ = 74.17) with mixed corona, containing both solvophilic and thermoresponsive units, with preferential aggregation number N_{ag} = 12 are obtained. One can observe that this aggregation number is smaller than the respective N_{ag} of $A_{30}B_{30}C_{15}$ terpolymers. The reason is the higher steric interactions in the micelle's corona in the case of $A_{30}B_{30}C_{30}$ due to the longer thermoresponsive block. At $T^* = 3.0$ the size of the thermoresponsive block decreases and the Flory χ_{AC}

dx.doi.org/10.1021/ma2025573 | *Macromolecules* 2012, 45, 2570–2579

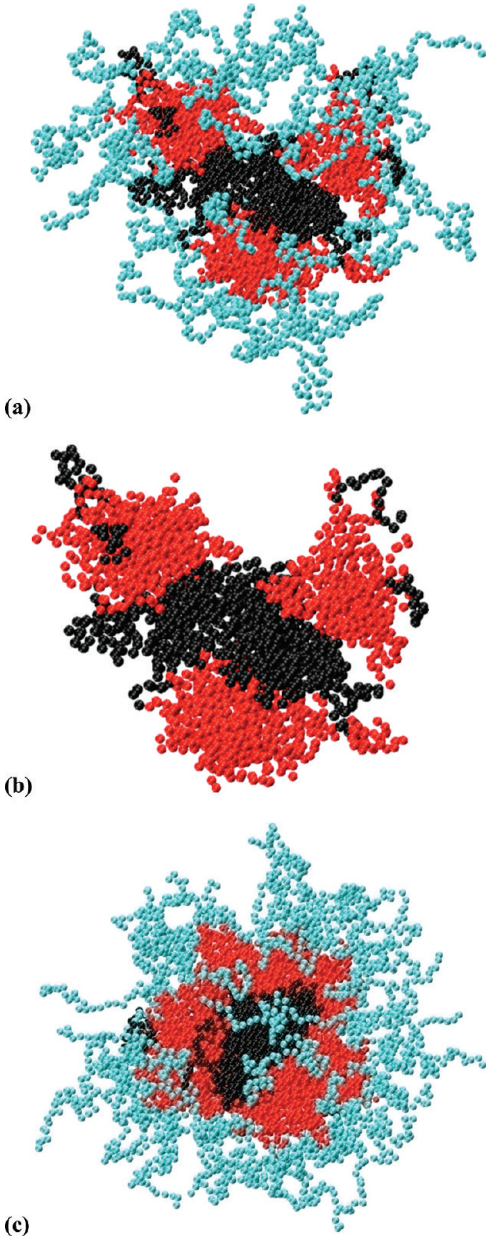

Figure 5. Snapshots of micelles formed by $A_{30}B_{30}C_{15}$ terpolymer with aggregation numbers (a) N_{ag} = 50 at T^* = 2.0, (b) N_{ag} = 50 at T^* = 2.0 with solvophilic beads excluded for clarity and (c) N_{ag} = 76 at T^* = 1.8.

parameter, describing the strength of A-C heterointeractions, increases. However, this increase is not high enough to change both the preferential aggregation number and the total size of micelles ($\langle R_g^2 \rangle$ = 74.31).

At solution temperatures T^* = 2.8 and 2.6 the preferential aggregation number increases to N_{ag} = 13 and 15 respectively, where the A-C heterointeractions become stronger. At this temperatures the thermoresponsive blocks occupy less space due to the decrease of their size but a small increase in the mean square radii of gyration of the whole micelle ($\langle R_g^2 \rangle_{mic}$) is observed ($\langle R_g^2 \rangle$ = 76.47, 80.32) due to the higher number of terpolymer chains involved in the aggregates. Temperature T^* = 2.4 triggers the aggregation of the thermoresponsive units as described in the $A_{30}B_{30}C_{15}$ case, driving the majority of terpolymer chains to form loose aggregates with N_{ag} varying

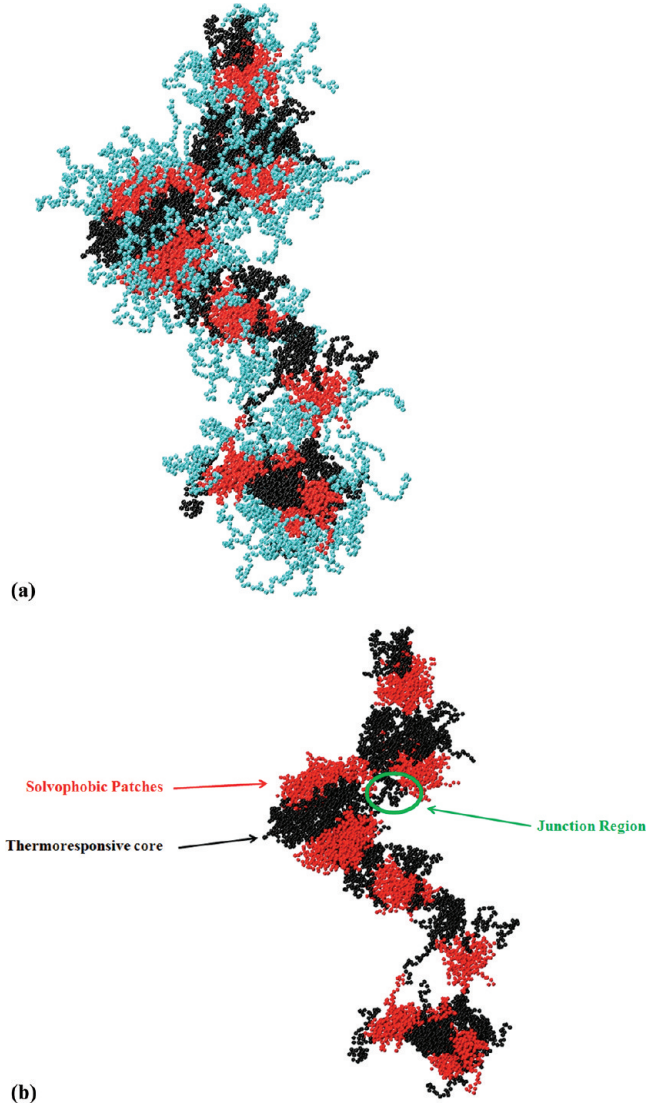

Figure 6. Snapshots of aggregates formed by $A_{30}B_{30}C_{30}$ terpolymer with N_{ag} = 122 at T^* = 2.4.

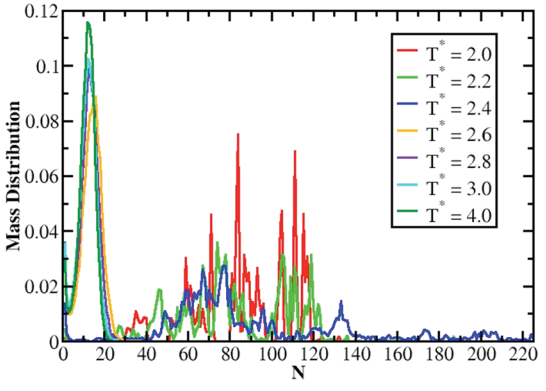

Figure 7. Mass distribution of aggregates for $A_{30}B_{30}C_{30}$ terpolymer at various solution temperatures T^*.

from 60 to 77. The shape of these micelles is spherical as indicated from the shape anisotropy parameter (κ^2 = 0.033 and 0.030) while the snapshot analysis revealed a raspberry-like mixed core with the thermoresponsive units lying in the interior and the solvophobic units residing, as patches, at the periphery

dx.doi.org/10.1021/ma2025573 | *Macromolecules* 2012, 45, 2570–2579

Table 2. Shape Characteristic Properties for $A_{30}B_{30}C_{30}$ Terpolymer Aggregates[a]

T^*	N_{ag}	$\langle R_g^2\rangle_{mic}$	$\langle R_g^2\rangle_{solvophobic}$	$\langle R_g^2\rangle_{thermoresponsive}$	$\langle \kappa^2\rangle_{mic}$	$\langle \kappa^2\rangle_{solvophobic}$	$\langle \kappa^2\rangle_{thermoresponsive}$
4.0	12	74.17 (0.09)	19.87 (0.08)	89.1 (0.3)	0.0279 (0.0007)	0.097 (0.002)	0.097 (0.002)
3.0	12	74.3 (0.2)	20.7 (0.1)	83.0 (0.5)	0.0298 (0.0007)	0.104 (0.003)	0.127 (0.003)
2.8	13	76.5 (0.1)	21.8 (0.1)	81.8 (0.7)	0.0282 (0.0004)	0.106 (0.003)	0.137 (0.003)
2.6	15	80.3 (0.5)	24.1 (0.2)	75.7 (1.3)	0.026 (0.001)	0.116 (0.004)	0.152 (0.005)
2.4	67	212.2 (21.5)	172.3 (20.4)	109.3 (33.3)	0.04 (0.04)	0.07 (0.05)	0.12 (0.09)
2.4	77	221.0 (15.6)	180.5 (14.9)	106.8 (21.9)	0.03 (0.03)	0.05 (0.04)	0.11 (0.07)
2.2	74	198.6 (1.6)	162.4 (2.0)	73.3 (1.5)	0.017 (0.005)	0.030 (0.009)	0.054 (0.007)
2.2	119	258.6 (21.8)	220.7 (21.9)	108.3 (25.8)	0.020 (0.005)	0.030 (0.005)	0.09 (0.03)
2.0	84	221.6 (33.20)	187.7 (33.9)	86.3 (38.7)	0.10 (0.05)	0.10 (0.05)	0.10 (0.05)
2.0	111	235.6 (1.0)	199.9 (1.0)	80.7 (1.1)	0.008 (0.002)	0.013 (0.002)	0.041 (0.008)

[a]Standard deviation is inside the parentheses.

of the core. A significant part of amphiphilic chains, around 29%, forms segmented worm like aggregates with $N_{ag} > 100$. The difference with the respective segmented worm like aggregates formed by the $A_{30}B_{30}C_{15}$ (Figure 4) terpolymers at the same solution temperature is found in the segmented worm-like structure (Figure 6a).

The building blocks of the segmented worm like structures are spherical micelles having raspberry-like mixed core with the thermoresponsive units lying in the interior and the solvophobic units residing, as patches, at the periphery of the core. These segments are connected to each other via thermoresponsive moieties as can be observed in Figure 6b. In the case of the $A_{30}B_{30}C_{15}$ terpolymers each segment core is composed by solvophobic units with two thermoresponsive stickers at the opposite sites of the periphery (Figure 4).

At $T^* = 2.2$, 2.0, and 1.8 only spherical micelles with similar raspberry-like core structure to the ones at $T^* = 2.4$ were obtained. At the solution temperature $T^* = 2.2$ the preferential aggregates contain 74 and 119 terpolymer chains, while when the temperature decreases at $T^* = 2.0$, N_{ag} becomes 84 and 111 respectively. At $T^* = 1.8$ all terpolymer chains were associated in micelles and no free chains were present in the solution. The lack of free chains is reflected on the shape of the mass distribution curve (not shown in the Figure 7) which becomes discontinuous with Dirac δ function type artifact peaks.

In order to study in detail the effects of the length of the thermoresponsive block on micelles hyper structures we are concentrated on the two different solution temperatures, $T^* = 2.4$ and 2.0 in which loose aggregates and normal micelles are formed, respectively.

3.3. Solution Temperature $T^* = 2.4$. Terpolymers $A_{30}B_{30}C_3$, $A_{30}B_{30}C_5$, $A_{30}B_{30}C_{10}$, and $A_{30}B_{30}C_{45}$ were also simulated at the solution temperature $T^* = 2.4$ and our results for the micelles mass distributions are illustrated in Figure 8, while the micelles' shape results are presented in Table 3. From Table 3, we can observe that the $A_{30}B_{30}C_3$ terpolymers form single spherical micelles ($\kappa^2 = 0.037$, $\langle R_g^2\rangle = 81$) with preferential aggregation number $N_{ag} = 21$ (Figure 8). Snapshot analysis indicated that the thermoresponsive blocks are located at the periphery of the solvophobic core segregated from each other forming very few aggregative domains. The thermoresponsive units are very well protected from the solvent by the solvophilic blocks and no secondary aggregation takes place. By increasing the length of thermoresponsive moiety ($A_{30}B_{30}C_5$ and $A_{30}B_{30}C_{10}$) we obtained similar results. The micelles aggregation number decreases to N_{ag} =20 and 17 respectively while a small decrease in the size of the spherical micelles ($\kappa^2 = 0.040$, $\kappa^2 = 0.040$) is also observed ($\langle R_g^2\rangle = 80$, $\langle R_g^2\rangle = 77$). In

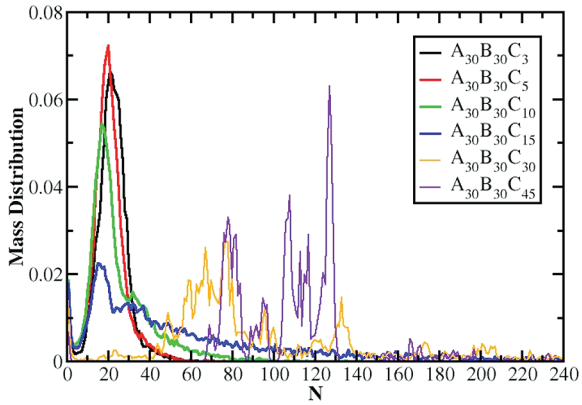

Figure 8. Mass distribution of aggregates for various ABC terpolymers at solution temperature $T^* = 2.4$.

micelles formed by $A_{30}B_{30}C_5$ terpolymers we observed an increased number of domains containing thermoresponsive units belonging to different terpolymers chains in the periphery of solvophobic core. Further increase of the thermoresponsive length ($A_{30}B_{30}C_{15}$) triggers the secondary aggregation of the single micelles as we have mentioned in the respective section and segmented worm-like hyper structures were obtained. In the case of $A_{30}B_{30}C_{30}$ terpolymers, the case analyzed in detail previously, spherical micelles with raspberry-like mixed core occupied the 70% of the total aggregation mass along with a 30% of segmented worms.

Terpolymers with longer thermoresponsive block ($A_{30}B_{30}C_{45}$) formed spherical micelles with aggregation numbers N_{ag} =78, 108, and 127 and only a 3% of segmented worms with segment structure similar to the one obtained in the case of $A_{30}B_{30}C_{30}$ terpolymers. Simulations of terpolymers with higher thermoresponsive content ($A_{30}B_{30}C_{60}$, $A_{30}B_{30}C_{90}$) suffered from the absence of free terpolymers chains. Nevertheless, snapshot analysis (Figure 9) indicates the formation of spherical micelles with raspberry-like core similar to the ones obtained in the case of the $A_{30}B_{30}C_{30}$, $A_{30}B_{30}C_{45}$ but with much greater aggregation numbers.

3.4. Solution Temperature $T^* = 2.0$. Our results for the $A_{30}B_{30}C_3$, $A_{30}B_{30}C_5$, $A_{30}B_{30}C_{10}$, $A_{30}B_{30}C_{15}$, and $A_{30}B_{30}C_{30}$ terpolymers are presented in Figures 10 and 11 and Tables 1, 2, and 3. From snapshot analysis and the values of shape anisotropy parameter κ^2, we observed a similar transition in the shape of micelles from spherical to segmented worm-like hyperstructures and back to spherical micelles, when the length of the thermoresponsive block increases. The difference with $T^* = 2.4$ is that the decrease of the solution temperature down

dx.doi.org/10.1021/ma2025573 | Macromolecules 2012, 45, 2570–2579

Table 3. Shape Characteristic Properties for Various Terpolymer Systems[a]

terpolymer	T^*	N_{ag}	$\langle R_g^2\rangle_{mic}$	$\langle R_g^2\rangle_{solvophobic}$	$\langle R_g^2\rangle_{thermoresponsive}$	$\langle \kappa^2\rangle_{mic}$	$\langle \kappa^2\rangle_{solvophobic}$	$\langle \kappa^2\rangle_{thermoresponsive}$
$A_{30}B_{30}C_3$	2.0	22	84.3 (0.5)	32.5 (0.5)	53.8 (0.5)	0.039 (0.002)	0.125 (0.009)	0.079 (0.006)
$A_{30}B_{30}C_3$	2.4	21	81.0 (0.4)	30.5 (0.3)	52.0 (0.2)	0.037 (0.002)	0.114 (0.006)	0.075 (0.003)
$A_{30}B_{30}C_5$	2.4	20	80.1 (0.5)	30.2 (0.4)	56.7 (0.4)	0.040 (0.003)	0.123 (0.007)	0.078 (0.003)
$A_{30}B_{30}C_5$	2.0	21	83.5 (0.5)	32.1 (0.5)	58.2 (0.4)	0.041 (0.002)	0.129 (0.008)	0.080 (0.004)
$A_{30}B_{30}C_{10}$	2.0	20	85.7 (1.4)	34.6 (1.4)	65.5 (0.9)	0.052 (0.007)	0.16 (0.02)	0.105 (0.007)
$A_{30}B_{30}C_{10}$	2.4	17	76.9 (1.2)	28.6 (1.2)	62.6 (1.3)	0.041 (0.003)	0.126 (0.009)	0.091 (0.004)
$A_{30}B_{30}C_{45}$	2.4	78	226.3 (7.3)	212.8 (8.0)	103.8 (7.0)	0.019 (0.009)	0.03 (0.01)	0.06 (0.03)
$A_{30}B_{30}C_{45}$	2.4	108	266.0 (5.1)	256.3 (5.4)	123.9 (6.8)	0.012 (0.005)	0.016 (0.006)	0.05 (0.02)
$A_{30}B_{30}C_{45}$	2.4	127	287.1 (10.3)	278.3 (10.5)	137.6 (11.4)	0.030 (0.005)	0.030 (0.005)	0.12 (0.09)

[a]Standard deviation is inside the parentheses.

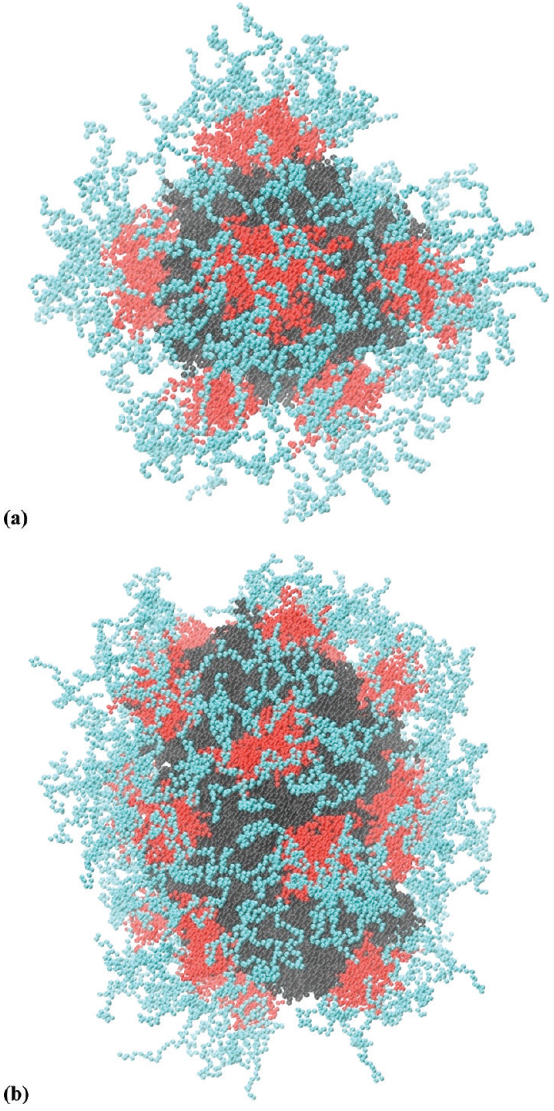

Figure 9. Snapshots of micelles formed by (a) $A_{30}B_{30}C_{60}$ terpolymer with aggregation number N_{ag} = 144 and (b) $A_{30}B_{30}C_{90}$ terpolymer with N_{ag} = 66 at T^* = 2.0.

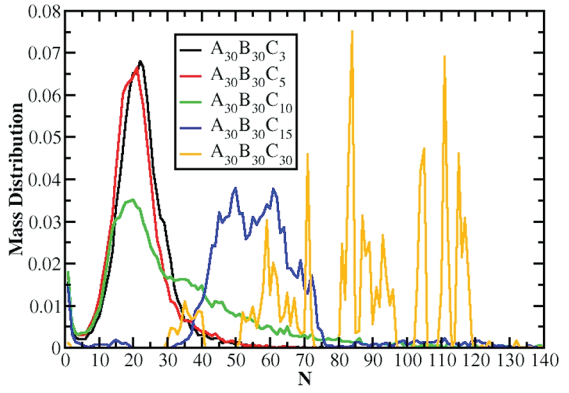

Figure 10. Mass distribution of aggregates for various ABC terpolymers at solution temperature T^* = 2.0.

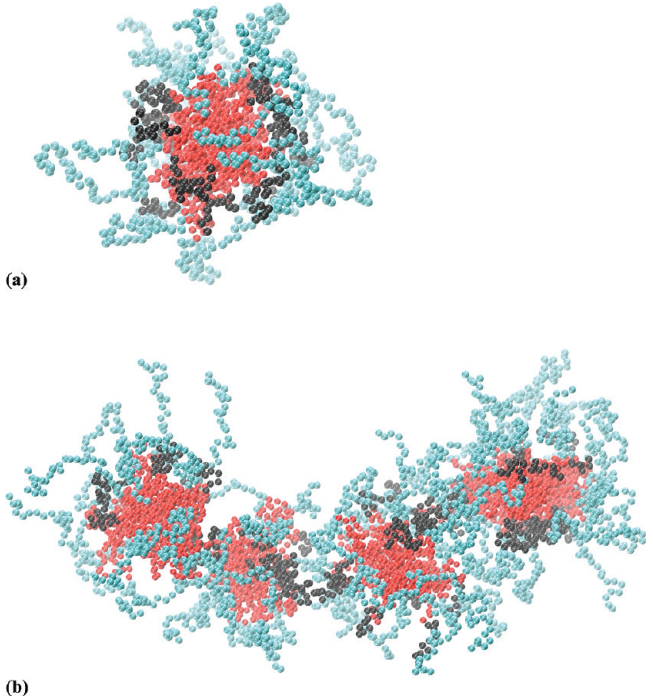

Figure 11. Snapshots of micelles formed by $A_{30}B_{30}C_{10}$ terpolymer with aggregation numbers (a) N_{ag} = 20 and (b) N_{ag} = 66 at T^* = 2.0.

to T^* = 2.0 triggers the formation of segmented worm hyperstructures in terpolymers with shorter thermoresponsive block ($A_{30}B_{30}C_{10}$). The comparison of the size of spherical micelles formed by terpolymers with short thermoresponsive length (smaller than the critical length that triggers the formation of segmented worm hyperstructures), e.g., $A_{30}B_{30}C_5$ with the same aggregation number N_{ag} = 20 at temperatures T^* = 2.4 and T^* = 2.0 showed a marginal decrease in the radius of gyration from $\langle R_g^2\rangle$ = 81.5 to $\langle R_g^2\rangle$ = 80.11 respectively. For terpolymers with thermoresponsive block greater than the aforementioned critical length, the differences in the size of micelles are much greater ($A_{30}B_{30}C_{30}$

dx.doi.org/10.1021/ma2025573 | Macromolecules 2012, 45, 2570−2579

in $T^* = 2.4$ has $N_{ag} = 49$, $\langle R_g^2 \rangle = 178$ and $\kappa^2 = 0.07$ while in $T^* = 2.0$ has $N_{ag} = 49$, $\langle R_g^2 \rangle = 159$ and $\kappa^2 = 0.05$) as expected. Hence, one can observe that the micelles obtained in $T^* = 2.0$ are smaller and more spherical.

4. COMPARISON WITH THE EXPERIMENTS

As we have mentioned in the Introduction, the micellization properties of PEO−PnBuA−PNiPAAm terpolymers were studied experimentally by Walther et al.[19] at the solution temperature of 45 °C. At this temperature, water is good solvent for the PEO block and bad solvent for PnBuA and the thermoresponsive PNiPAAm blocks. In all samples PEO blocks contained 114 monomers while the PNiPAAm blocks contained a varying number of monomers equal to 65, 82, 116, 165, 178, 197, and 350. By straightforward calculations we have determined the number of segments and the Kuhn length of PEO block using the characteristic ratio value $C_\infty = 4.055$.[26,27] Similarly we have calculated the number of PNiPAAm segments using the PNiPAAm Kuhn length value of 0.7 nm, obtained from the literature.[28] We found that the terpolymers studied by Walther et al.[19] contained 20 PEO segments having Kuhn length equal to 1.339 nm and 10, 21, 30, 32, 35, and 63 PNiPAAm segments with almost half the Kuhn length. Thus, the experimental terpolymers would be equivalent to our $A_{40}B_xC_{10}$, $A_{40}B_xC_{21}$, $A_{40}B_xC_{30}$, $A_{40}B_xC_{32}$, $A_{40}B_xC_{35}$, and $A_{40}B_xC_{63}$ which contains the longer thermoresponsive block with contour length 1.5 times larger than the respective length of the hydrophilic block. For the $A_{40}B_xC_{10}$ terpolymer they found that the temperature induced aggregation was clearly absent due to long PEO block that sufficiently shielded the collapsed PNiPAAm patches from aggregation. The $A_{40}B_{30}C_{21}$ and $A_{40}B_{30}C_{30}$ formed spherical or elongated sphere aggregates and appeared to have an increased total radius of gyration by 15% in comparison with the one at $T = 25$ °C (good solvent for the thermoresponsive block). For the $A_{40}B_{30}C_{32}$, $A_{40}B_{30}C_{35}$, and $A_{40}B_{30}C_{63}$ terpolymers, with long thermoresponsive block, segmented worm-like hyperstructures were formed. The authors[19] considering the size of the PEO and PNiPAAm monomers instead of the Kuhn lengths concluded that the thermoresponsive block was 3 times longer than the hydrophilic one. Consequently they concluded that Janus type aggregation (with one aggregative thermoresponsive patch) does not take place in the case of thermoresponsive terpolymers because for such long thermoresponsive blocks spherical micelles were not observed (see Figure 6e of ref 29).

Our simulation results for both solution temperatures $T^* = 2.0$ and 2.4 clearly indicate a micelle shape transition from spheres to segmented worms and to spheres again. Our results are in qualitative agreement with the experimental results for ABC miktoarm star terpolymers composed by two hydrophobic (poly(ethylethylene), poly(methylcaprolactone)) and one hydrophilic (poly(ethylene oxide)) branches, studied by Li et al.[20] According to our experience the micelle shape obtained from linear and three arm star copolymers[6,8] (consist of one or two solvophobic blocks) are quite similar, differ in the preferential aggregation number (micelle size). The linear ABC terpolymer contains two successive blocks under bad solvent conditions behave as a linear diblock copolymer with a solvophilic and solvophobic block. Thus, the micellization of linear ABC terpolymers should be similar to respective star ABC terpolymers.

As we have mentioned in the introduction, Li et al.[20] found that when the poly(methylcaprolactone) arm increases, a transition from spherical micelles to segmented worm hyperstructures and back to spherical micelles takes place. Since both experimental systems are very similar in bad solvent conditions we suppose that PEO−PnBuA−PNiPAAm terpolymers with even larger PNiPAAm blocks should form spherical micelles as we found in our simulations. Further experimental studies are needed to clarify this issue.

5. OTHER APPROACHES IN MODELING OF THERMORESPONSIVE POLYMERS

The coil to globule transition of a single PNIPAM homopolymer chain was studied experimentally by laser light scattering techniques in an extremely dilute aqueous solution.[30] The radius of gyration of the PNIPAM chain indicates a sharp coil to globule transition, reaching its fully collapsed globule state before demixing. Our simulations for the coil to globule transition of a single polymer chain, using a typical Lennard-Jones potential predict a gradual shrinking of the polymer chain even after the solution enters inside the binodal region, as shown in Figure 12. Similar results are also obtained by other existing models using the typical Lennard-Jones potential.

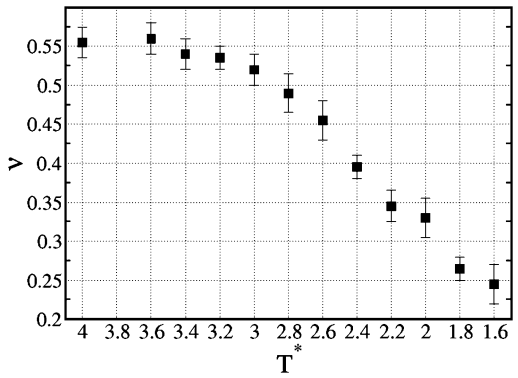

Figure 12. Critical exponent, ν, of the mean radius of gyration ($\langle S^2 \rangle \sim N^{2\nu}$) for a single polymer chain versus the reduced solution temperature, T^*.

Anderson et al.[31] separated thermal effects into kinetic temperature and solvation effects, which has allowed parametrizing of the temperature by a single parameter α in an implicit solvent coarse grained model. The potential used is a modified Lennard-Jones to describe the interactions between units

$$U(r_{ij}) = 4\varepsilon_{ij}\left[\left(\frac{\sigma}{r_{ij}}\right)^{12} - a\left(\frac{\sigma}{r_{ij}}\right)^{6}\right] \quad (6)$$

The parameter α varies between $0 \leq \alpha \leq 1$. This way the variation of the radius of gyration critical exponent ν (Figure 4 of ref 31), for long polymer chains, mimics better the experimental findings (more abrupt coil to globule transition and constant values of ν inside the binodal region) and should be efficient for the study of the thermoresponsive polymers.

6. CONCLUSIONS

The micellization behavior of linear ABC terpolymers containing a solvophobic block in the middle, accompanied by solvophilic and thermoresponsive blocks at the ends, was studied by means of Brownian dynamics simulations. The

dx.doi.org/10.1021/ma2025573 | Macromolecules 2012, 45, 2570−2579

effects of the length of the thermoresponsive moiety on the shape and size of aggregates, formed as the temperature of the solution reduces and solvent progressively becomes bad for the thermoresponsive block, were studied in detail. Analysis of the radius of gyration of the thermoresponsive block of single chain terpolymers revealed the existence of different crossover solution temperatures, $T^* = 2.4$ and $T^* = 2.0$, corresponding to the formation of loose aggregates and regular micelles. At both temperatures, as the length of thermoresponsive block increases, we found a shape transition from spherical to segmented worm-like and back to spherical loose aggregates or micelles.

Our results are in qualitative agreement with the experimental findings on star ABC terpolymers with one hydrophilic and two hydrophobic branches. Walther et al. studied similar linear ABC terpolymers and observed a shape transition of micelles from spherical to segmented worm-like, as the length of thermoresponsive block increases. Our analysis on their terpolymer Kuhn lengths, and our simulation results, may suggest that in order the PEO−PnBuA−PNiPAAm terpolymers to reach the full shape transition from spherical to segmented worm-like and back to spherical micelles, longer thermoresponsive length PNiPAAm blocks are needed.

AUTHOR INFORMATION

Corresponding Author

*E-mail: cvlahos@cc.uoi.gr.

Notes

The authors declare no competing financial interest.

ACKNOWLEDGMENTS

The Research Center for Scientific Simulations (RCSS) of the University of Ioannina is gratefully acknowledged for providing the computer resources used in this work. We thank the reviewer who brought to our notice ref 31.

REFERENCES

(1) Rodriguez-Hernandez, J.; Checot, F.; Gnanou, Y.; Lecommandoux, S. *Prog. Polym. Sci.* **2005**, *30*, 691−724.
(2) Hadjichristidis, N.; Pispas, S.; Floudas, G. Block Copolymers, Synthetic Strategies. In *Physical Properties and Applications*; Wiley-Interscience: Hoboken, NJ, 2003.
(3) Iatrou, H.; Willner, L.; Hadjichristidis, N.; Halperin, A.; Richter, D. *Macromolecules* **1996**, *29*, 581−591.
(4) Mountrichas, G.; Mpiri, M.; Pispas, S. *Macromolecules* **2005**, *38*, 940−947.
(5) Nguyen, P.; Hammond, P. *Langmuir* **2006**, *22*, 7825−7832.
(6) Cheng, L.; Cao, D. *Langmuir* **2009**, *25*, 2749−2756.
(7) Moultos, O.; Gergidis, L. N.; Vlahos, C. *Macromolecules* **2010**, *43*, 6903−6911.
(8) Georgiadis, C.; Moultos, O.; Gergidis, L. N.; Vlahos, C. *Langmuir* **2011**, *27*, 835−842.
(9) Taribagil, R. R.; Hillmyer, M. A.; Lodge, T. P. *Macromolecules* **2010**, *43*, 5396−5404.
(10) Charbonneau, C.; Chassenieux, C.; Colombani, O.; Nicolai, T. *Macromolecules* **2011**, *44*, 4487−4495.
(11) Cui, J.; Jiang, W. *Langmuir* **2010**, *26*, 13672−13676.
(12) Charlaganov, M.; Borisov, O. V.; Leermarkers, F. A. M. *Macromolecules* **2008**, *41*, 3668−3677.
(13) Eisenberg, A.; Yu, G. E. *Macromolecules* **1998**, *31*, 5546−5549.
(14) Berlpsch, H.; Bottcher, C.; Skrabania, K.; Laschewsky, A. *Chem. Commun.* **2009**, 2290−2292.
(15) Zhang, L.; Bernard, J.; Davis, T. P.; Barner-Kowollik, C.; Stenzel, M. H. *Macromol. Rapid Commun.* **2008**, *29*, 123−129.
(16) Gu, J.; Cheng, W. P.; Liu, J.; Lo, S. Y.; Smith, D.; Qu, X.; Yang, Z. *Biomacromolecules* **2008**, *9*, 255−262.
(17) Sfika, V.; Tsitsilianis, C.; Kiriy, A.; Gorodyska, G.; Stamm, M. *Macromolecules* **2004**, *37*, 9551−9560.
(18) Zhao, J.; Zhang, G.; Pispas, S. *J. Polym. Sci., Part A: Polym. Chem* **2009**, *47*, 4099−4110.
(19) Walther, A.; Barner-Kowollik, C.; Müller, A. H. E. *Langmuir* **2010**, *26*, 12237−12246.
(20) Li, Z.; Hillmyer, M. A.; Lodge, T. P. *Langmuir* **2006**, *22*, 9409−9417.
(21) Suek, N.; Lamm, M. *Langmuir* **2008**, *24*, 3030−3036.
(22) Murat, M.; Grest, G. *Macromolecules* **1996**, *29*, 1278−1285.
(23) LAMMPS Molecular Dynamics Simulator http://lammps.sandia.gov. Accessed 11/2011.
(24) Plimpton, S. J. *Comput. Phys.* **1995**, *117*, 1−19.
(25) Yan, J.; Ji, W.; Chen, E.; Li, Z.; Liang, D. *Macromolecules* **2008**, *41*, 4908−4913.
(26) Zhang, W.; Zou, S.; Wang, C.; Zhang, X. *J. Phys. Chem. B* **2000**, *104*, 10258−10264.
(27) Lee, H.; Venable, R. M.; MacKerell, A. D. Jr.; Pastor, R. W. *Biophys. J.* **2008**, *95*, 1590−1599.
(28) Rodd, L. E.; Scott, T. P.; Cooper-White, J. J.; McKinley, G. H. *Appl. Rheol.* **2005**, *15*, 12−27.
(29) Sheng, Y.-J.; Nung, C.-H.; Tsao, H.-K. *J. Phys. Chem. B* **2006**, *110*, 21643−21650.
(30) Wang, X.; Qiu, X.; Wu, C. *Macromolecules* **1998**, *31*, 2972−2976.
(31) Anderson, A. J.; Travesset, A. *Macromolecules* **2006**, *39*, 5143−5151.